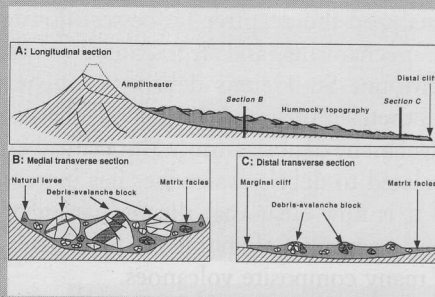


# DEBRIS AVALANCHES

TADAHIDE UI  
*Hokkaido University*

SHINJI TAKARADA  
*Geological Survey of Japan*

MITSUHIRO YOSHIMOTO  
*Hokkaido University*



- I. Introduction
- II. Geomorphic Characteristics
- III. Internal Framework
- IV. Frequency and Magnitude
- V. Eruption Processes
- VI. Flow and Emplacement Processes
- VII. Examples
- VIII. Conclusions

## GLOSSARY

**amphitheater** An arm-chair-shaped landscape formed at the source of a sector collapse. The depth, width, and height of an amphitheater are variable. Amphitheaters associated with a major debris avalanche at composite volcanoes may enclose the summit vent.

**debris avalanche** The product of a large-scale collapse of a sector of a volcanic edifice under water-undersaturated conditions. The deposit is characterized by two depositional facies, "block" and "matrix." An amphitheater at the source and hummocky topography on the surface of the deposit are characteristic topographic features of a debris avalanche.

**debris-avalanche block** A fractured and deformed piece of the source volcano included within a debris avalanche deposit. The sizes of single blocks are variable, more

than several hundred meters across as a maximum and less than a meter across as a minimum.

**debris-avalanche matrix** A debris-avalanche matrix is a mixture of small volcanic clasts derived from various parts of the source volcano. This facies is massive, poorly sorted, and made of fragments of volcanoclastic formations and occasionally of fragments of paleosols and plants.

**hummocks** Characteristic topographic features for debris avalanche deposits. The shape of hummocks is variable and irregular. No overall trend in the alignment of hummocks is found.

**jigsaw cracks** Jigsaw cracks are characteristic joint patterns within a debris-avalanche block. Jigsaw cracks are typically more irregular than the cooling joints of massive igneous rocks. The joint planes usually remain closed, but many of them open wide due to deformation during the transport of the debris avalanche.

**sector collapse** A destructive volcanic process during the growth history of a volcano. Debris avalanche deposits are the products of sector collapses.

**A** SECTOR COLLAPSE of a volcanic edifice produces a debris avalanche. A debris avalanche is triggered typically by intrusion of new magma, a phreatic explosion, or an earthquake. A debris avalanche is generated at water-undersaturated conditions. The

deposit is characterized by two depositional facies, the debris-avalanche block and the debris-avalanche matrix facies. The debris-avalanche block facies is composed of large, coherent yet fractured and deformed pieces of the source volcano that formed the debris avalanche deposit. The debris-avalanche matrix facies is a more uniform and fine-grained mixture of volcanic fragments derived from various parts of the source volcano. An amphitheater at the source and hummocky topography on the surface of the deposit are characteristic topographic features produced by a debris avalanche.

texture, internal structure, or surface morphology. Scientists from the United States Geological Survey (USGS) analyzed the eruptive processes, flowage, emplacement mechanisms, and depositional structure for the 1980 Mount St. Helens debris avalanche. Other researchers then summarized the general characteristics of debris avalanche deposits. Since this critical eruption, research related to debris avalanches has increased significantly. It is now clear that the formation of debris avalanches is a common phenomenon within the growth history of many composite volcanoes.

## I. INTRODUCTION

Debris avalanches are recently recognized volcanic phenomena. One of the recent historical events was when the northern sector of Mount St. Helens collapsed to be emplaced as a debris avalanche deposit in the upper tributary of Toutle River on May 18, 1980. Similar processes were observed and recorded during the 1888 eruption of Bandai in Japan and the 1956 eruption of Bezymianny in Kamchatka. These events were first classified as ultravulcanian eruptions until their true nature was understood. Before the eruption of Mount St. Helens in 1980, most debris avalanche deposits were interpreted as lahar deposits. Some other debris avalanche deposits have been interpreted as pyroclastic flow deposits, lava flows, or moraines, due to the similarities in

## II. GEOMORPHIC CHARACTERISTICS

Hummocky topography, natural levees, a marginal cliff, and an amphitheater at the source are characteristic geomorphic features of a debris avalanche deposit (Fig. 1). Hummocky topography is perhaps the most significant geomorphic feature. The shape of individual hummocks is variable and irregular (Fig. 2A). Although parallel alignments of the long axes of hummocks have been described in some deposits, no consistent overall trend has been observed. The volume and height of hummocks are larger in the proximal to medial part of the deposit and decrease toward the distal end. Some glacial terminal moraines show a similar topographic expression. Due to irregularity in form and composition, it is often

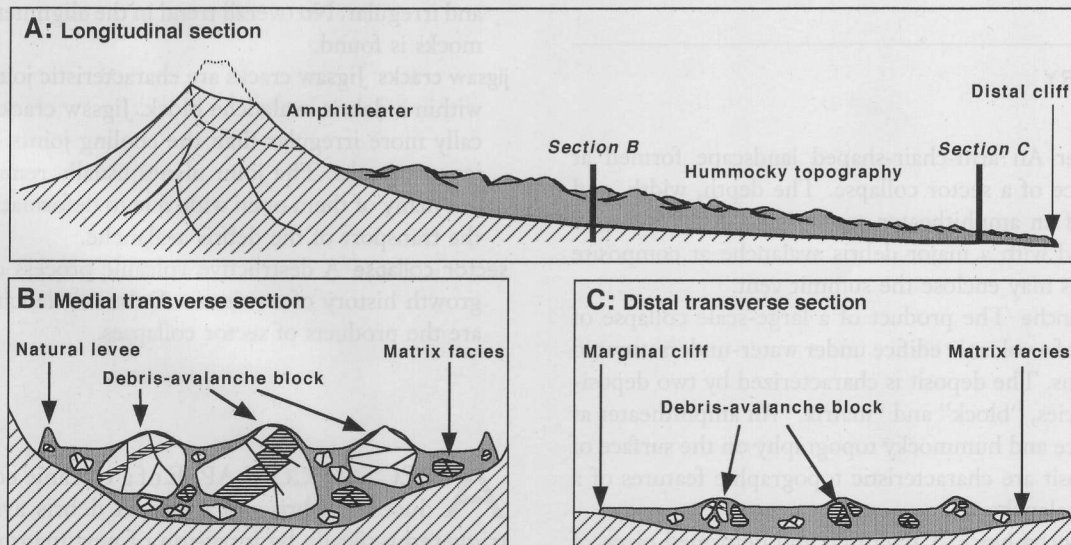


FIGURE 1 Schematic section for a debris avalanche deposit: (A) a longitudinal section stretching from the source amphitheater to the distal end; (B) a transverse section of the medial region; (C) a transverse section for the distal region. Size of hummocks gradually decreases toward the distal area. Debris-avalanche blocks are smaller and scarce at the distal area.

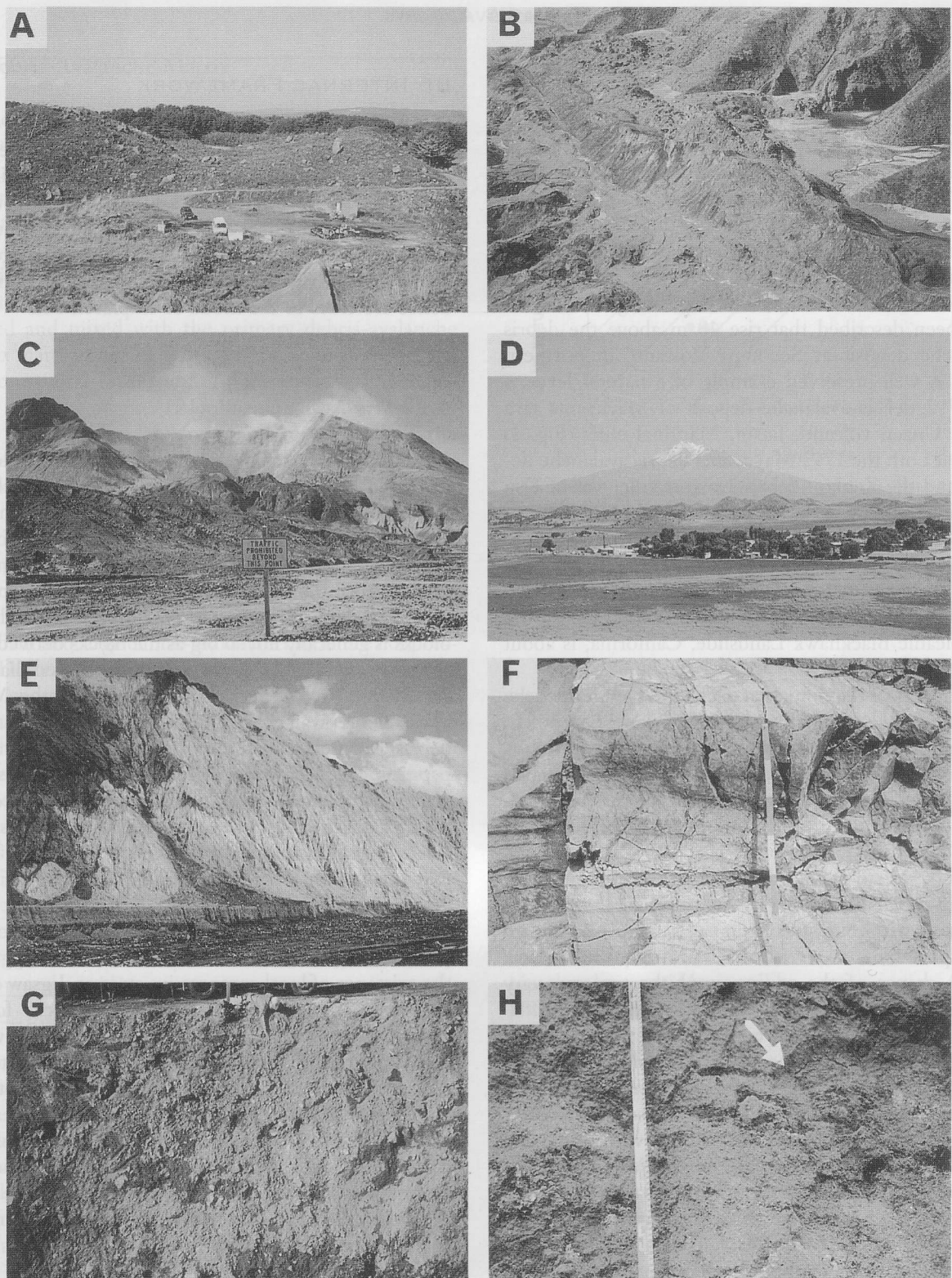


FIGURE 2 Photographs of debris avalanche features: (A) hummocky topography, 466 B.C. Kisakata debris avalanche deposit, Chokai volcano, northern Japan; (B) natural levee in the medial region of the 1980 Mount St. Helens debris avalanche deposit; (C) amphitheater of the 1980 Mount St. Helens debris avalanche; (D) hummocky terrain and a source region already filled with post-avalanche volcanic deposits, Mount Shasta; (E) a section of a debris-avalanche block, 1980 Mount St. Helens deposit; (F) a jigsaw crack, Owarabi debris avalanche deposit, Chokai volcano, Japan; (G) a section of debris-avalanche matrix, 466 B.C. Kisakata debris avalanche deposit, Chokai volcano, northern Japan; (H) deformed soft soil fragments (arrow) near the bottom contact of the 1792 debris avalanche deposit, Unzen volcano, Japan.

hard to discriminate debris avalanche deposits based on topography alone. Internal depositional features should be examined to confirm the origin of a deposit. Similar undulating topography is also known in the case of small-scale pyroclastic flow deposits. However, their gentle and regularly undulating pattern differs from the hummocky topography of debris avalanche deposits.

Natural levees (Fig. 2B), a marginal cliff, and a distal cliff are other characteristic topographic features in a well-preserved debris avalanche deposit. Natural levees have been described that rise 40 m above the debris avalanche deposit at Socompa Volcano, in northern Chile. A well-preserved example of a natural levee is the 1792 debris avalanche deposit of Mayuyama lava dome, Unzen volcano, Japan. Marginal cliffs (Fig. 1) occur at both the 1792 Mayuyama debris avalanche deposit and the Zenkoji debris avalanche deposit of Usu volcano, Japan. The height of marginal cliffs is up to 10 m. The cliffs develop at the lower part of a debris avalanche deposit if it is emplaced on a wide plain. Distal cliffs are a continuation of the marginal cliff at the distal end of the deposit. The height of the distal cliff at the nonvolcanic Blackhawk Landslide, California, is about 20 m.

Remnants of temporary river channels are left on the surface of the valley-filling debris avalanche deposits. Typical examples of this are seen at the Kusakata debris avalanche of Chokai volcano and the Nirasaki debris avalanche of Yatsugatake volcano in Japan. Such phenomena form soon after the emplacement of the debris avalanche. In the case of the 1980 Mount St. Helens eruption, stream capture began just after the emplacement of the debris avalanche and the river channel had stabilized within several years after emplacement of the deposit.

The shapes of the source amphitheaters can vary widely. The amphitheater formed during the 1980 Mount St. Helens debris avalanche is a fairly typical example, showing a U-shaped plan view (Fig. 2C). The floor slopes northward toward the opening (Fig. 1). The initially steep wall of the amphitheater has slumped now to form a lower gradient apron. The growth of a central lava dome partially has filled the amphitheater (Fig. 2C). Ultimately, lava flows and dome growth will fill the amphitheater as seen at Mount Taranaki in New Zealand and Mount Shasta (Fig. 2D) and Mount Rainier in the United States. Amphitheaters can also be formed by relatively small-scale debris avalanches on the outer slope of a volcanic edifice, as in the case of the 1792 Mayuyama debris avalanche at Unzen volcano. These amphitheaters show relatively wide angles and shallow depths.

### III. INTERNAL FRAMEWORK

The internal framework of debris avalanche deposits comprises debris-avalanche blocks and a debris-avalanche matrix. Debris-avalanche blocks are surrounded by a debris-avalanche matrix. Fracture patterns and fault displacement in debris-avalanche blocks, heterogeneity in the debris-avalanche matrix, and paleomagnetic evidence are clues to the mode of emplacement.

#### A. Debris-Avalanche Blocks

Most debris-avalanche blocks are fragments derived from the source volcano (Fig. 2E). These blocks are fractured and deformed but preserve many of the primary textures and geologic structures of the source volcano. Some debris-avalanche blocks are fragments eroded from the ground surface during transportation of the avalanche. The size of such debris-avalanche blocks is generally not so big as the blocks derived from the source volcano. The maximum measured diameter for a debris-avalanche block is 280 m in the Mount Shasta debris avalanche deposit. The diameter of smaller debris-avalanche blocks may be less than 1 m. Fracture patterns called jigsaw cracks are commonly observed within debris-avalanche blocks (Fig. 2F). Jigsaw cracks within a debris-avalanche block are typically not as regular as the cooling joints of massive igneous rocks. These joint planes usually remain closed, but some of them open widely, due to deformation during transport of the debris avalanche. Conjugated joint patterns can form in the massive part of debris-avalanche blocks, suggesting the existence of local compressive stresses. Jigsaw cracks are common within debris-avalanche blocks formed from massive lava flows and dikes and are scarce within debris-avalanche blocks made of volcanoclastic materials. The frequency of jigsaw cracks depends on both the rock type and travel distance.

Some debris-avalanche blocks show minor fault displacements (Fig. 1). The paleomagnetic orientations of samples collected from a single debris-avalanche block are often nearly uniform. However, the declination varies between debris-avalanche blocks and differs from that of the source volcano. This implies that initial avalanche material split into many pieces and the rotation of large (>ca. 10 m) debris-avalanche blocks is only about an axis perpendicular to the ground surface. There is little or no rotation parallel to the ground surface.

## B. Debris-Avalanche Matrix

The debris-avalanche matrix consists of a mixture of smaller volcanic fragments derived from various parts of the source volcano (Fig. 2G). No jigsaw cracks develop within the debris-avalanche matrix. The paleomagnetic orientation of clasts in the matrix is random. This suggests that the debris-avalanche matrix is formed by the collision and fragmentation of debris-avalanche blocks. Fluvial gravels, soil layers, and basement rocks are eroded and mixed with the primary debris-avalanche matrix material during flowage. The abundance of such exotic material logarithmically increases with distance away from the source. Hummocks are mainly made of huge debris-avalanche blocks and surrounded by the debris-avalanche matrix. Smaller (<ca. 2 m) debris-avalanche blocks float within the debris-avalanche matrix (Fig. 1). The lithology of the debris-avalanche matrix is variable even within a large exposure scale.

The lithology within a few meters of the basal contact of a debris avalanche deposit differs from that of the other parts of the deposit. Fine-grained material is more abundant and large debris-avalanche blocks are not present. Deformed soft sediments are common near the basal contacts (Fig. 2H). This reflects higher shear strains at the base of flows.

"Block facies" and "matrix facies" are terms used to define mappable areas of a debris avalanche deposit. In the block facies many debris-avalanche blocks are assembled to form hummocky terrain. Matrix facies deposits contain a predominance of debris-avalanche matrix and are topographically flat (Fig. 1).

## IV. FREQUENCY AND MAGNITUDE

The largest Quaternary debris avalanche deposit known in the world is the 300- to 360-kyr-old Mount Shasta deposit in the United States. The collapse height for the deposit is estimated as 3500 m and the runout distance is at least 45 km. A database for Japanese Quaternary volcanoes includes 71 deposits from 52 volcanoes (Fig. 3) (Table I). The maximum runout distance ( $L$ ) ranges from 1.6 to 32 km, and the maximum collapse height ( $H$ ) ranges from 0.2 to 2.4 km. The ratio  $H/L$  is equivalent to the apparent coefficient of friction during sliding, or the slope of an energy cone for an eruption.  $H/L$  is generally between 0.2 and 0.06. The ratio is generally lower than that of nonvolcanic landslides of similar size. It has been

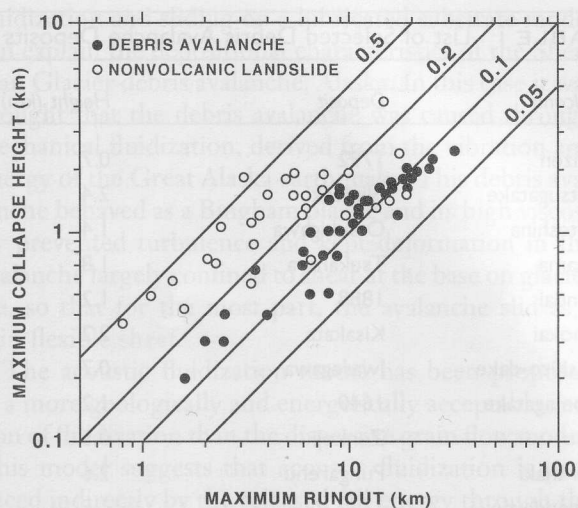


FIGURE 3 Relationship between the collapse height and runout distance for Japanese Quaternary debris avalanche deposits (solid circles) and nonvolcanic landslide deposits (open circles). The ratio of collapse height to runout distance for debris avalanche is generally between 1.2 and 0.06. It is possible to establish hazard zones for future debris avalanches using this ratio.

suggested that this greater mobility results either from the presence of fragmented volcanoclastic materials within a volcanic edifice or from phreatic explosions triggered by sudden decrease of the confining pressure at the time of sliding. Another possible cause of lower  $H/L$  is the more common occurrence of weak hydrothermally altered rocks within volcanoes.

Some debris avalanches transform during transport to clay-rich lahars and spread more widely than ordinary debris avalanches. The existence of long-runout debris avalanche deposits has been shown at Colima and Citlaltépetl volcanoes, Mexico. The source region for the latter is thought to be centered in hydrothermally altered materials in a water-saturated condition. The collapse started in an avalanche manner but transformed to a clay-rich cohesive lahar and moved an unusually long distance, over 120 km away from the source. Collapse height is assumed to be 3–4 km and its  $H/L$  ratio is 0.04. The Osceola Mudflow from Mount Rainier, United States, transformed from a debris avalanche only 2 km away from the source and traveled down to more than 120 km from its origin. The source material included a large volume of pore water and hydrothermally altered rock.

Debris avalanches are common phenomena during the entire growth history of composite volcanoes. The frequency of debris avalanches in the entire Japanese islands is, on average, about once per century. The fre-

TABLE 1 List of Selected Debris Avalanche Deposits

Volcano	Deposit	Height (km)	Length (km)	Volume (km <sup>3</sup> )	Type	Source
Unzen	1792	0.7	6	0.48	U	D
Yatsugatake	Nirasaki	2.4	32	9		S
Tateshina	Otsukigawa	1.4	12.5	0.35		S
Asama	Tsukahara	1.8	20	2		S
Bandai	1888	1.2	11	1.5	Ba	S
Chokai	Kisakata	2.2	25	3.5	Ba?	S
Tashiro-dake	Iwasegawa	0.7	8.8	0.55		S
Komagatake	1640	1.2	15	1.1	Bz	S
Usu	Zenkoji	0.5	6.5	0.3	Ba?	S
Taranaki	Pungarehu	2.6	31	7.5		S
Papandayan	1772	1.5	11	0.14		
Iriga	1628?	1.1	11	1.5		S
Banahao	Lucena and Lucban	1.7	26	5		S
Bezymianny	1956	2.4	18	0.8	Bz	S
Shiveluch	1964	2	12	1.5		S
St. Helens	1980	2.55	24	2.5	Bz	S
Shasta	300–360 kyr B.P.	3.55	50	26		S
Chaos Crags	ca. 1650	0.65	5	0.15		D
Citlaltépetl	Teteltzingo	4	85	1.8	L	S
Colima	Nevado de Colima	4.3	120	22–33	L	S
Socompa	Holocene	3	35	15	Bz	S
Rainier	Osceola	4.7	120	3.8	L	S

Abbreviations: Bz, Bezymianny type; Ba, Bandai type; U, Unzen type; L, long-runout debris avalanche; S, stratovolcano; D, lava dome.

quency of debris avalanches at each composite volcano is less than one per 10 kyr. Older debris avalanche deposits will generally be covered by younger deposits or eroded. Thus the exact frequency of debris avalanche events is often difficult to confirm.

## V. ERUPTION PROCESSES

The processes that form debris avalanches are variable. Three types of debris avalanches have been proposed: Bezymianny, Bandai, and Unzen types. Bezymianny-type debris avalanches are associated with magmatic eruptions, as in the case of Mount St. Helens in 1980. The Bandai type is associated with a phreatic eruption, as in the case of Bandai, Japan, in 1888. The duration of precursory phenomena associated with recorded ex-

amples is variable. No juvenile material is included within this type of deposit. The Unzen type is not directly related to volcanic activity, but triggered by an earthquake. Another origin for debris avalanches is slumping of a caldera wall during the process of caldera collapse. Major slope failure of oceanic islands also causes submarine debris avalanches.

The collapse process is not always simple as the case of Mount St. Helens in 1980. Two successive collapses creating two separate deposits also occurred during the 1640 debris avalanche of Hokkaido-Komagatake, Japan. In the case of the debris avalanche deposit of Banahao volcano, Philippines, two successive collapses occurred and flowed in different directions in the proximal area but merged into a single flow at the middle to distal area.

A lateral blast accompanied the 1980 Mount St. Helens debris avalanche and the 1956 debris avalanche of Bezymianny volcano. The lateral blasts spread over a much wider area than the debris avalanches and

destroyed a large area of forest. A lateral blast did not accompany the 1792 debris avalanche of Unzen volcano.

## VI. FLOW AND EMPLACEMENT PROCESSES

More than 20 dynamic emplacement models have been proposed to explain the high mobility of large volcanic and nonvolcanic debris avalanches and many controversies over their emplacement still continue. The air fluidization theory was proposed based on geologic relations of the Saidmarreh, Frank, and Madison debris avalanches as well as on eyewitness accounts of their emplacement. A "hovercraft" mechanism, involving air-layer lubrication, was proposed to explain the long runout and sedimentological and morphological features, for example, preserved intact primary stratigraphy, bulldozed distal ridges, three-dimensional jigsaw-puzzle breccia, distal rims, lateral levees, and transverse ridges and troughs, in the Blackhawk and Sharman debris avalanches, United States. However, the air-layer lubrication mechanism has difficulties in explaining debris avalanches on Mars and the Moon and subaqueous debris avalanches on Earth. A basal gaseous pore pressure model was proposed to explain the rapid velocities and low apparent angle of friction of large coherent debris avalanches using pore fluid vaporization along their bases due to frictional heating during sliding. A basal self-lubrication mechanism is an alternative explanation of the low angle of friction and other characteristic features of the Blackhawk debris avalanche. The Blackhawk debris avalanche bulldozed a distal heap of sandstone ahead of it as it progressed downslope at high speed. The sandstone "breccia" at the front of the flow was "smeared out" beneath the overriding marble breccia, providing a zone of high fluidity beneath the front of the debris lobe (self-lubrication).

A mechanical fluidization model based on the revived idea of grain contact linked with granular flow theory has also been suggested. This assumes the presence of an intergranular fluid and proposes that highly energetic interstitial dust could reduce the effective normal pressure on grains and consequently reduce frictional resistance. For wet debris avalanches, such as the 1970 Huascarán debris avalanche, it is thought that mud could have formed the fluid component between clasts. In the case of large dry debris avalanches, fine dust might act as the interstitial fluid. A combination of mechanical

fluidization and sliding on a lubricated substrate model can explain the depositional characteristics of the Sherman Glacier debris avalanche, Alaska. In this case it was thought that the debris avalanche was caused through mechanical fluidization, derived from the vibration and energy of the Great Alaska earthquake. This debris avalanche behaved as a Bingham plastic and its high viscosity prevented turbulence and kept deformation in the avalanche largely confined to shear at the base on glacier ice, so that for the most part, the avalanche slid as a thin flexible sheet.

The acoustic fluidization model has been proposed as a more geologically and energetically acceptable version of fluidization than the dispersive grain flow model. This model suggests that acoustic fluidization is produced indirectly by the released fall energy through the propagation of strong sound waves of just the right frequency through a flowing breccia stream. Acoustic fluidization requires much less energy than mechanical fluidization.

For debris avalanches composed of limestone, notably Films (Switzerland), another lubricated sliding model has been suggested. It is believed that high temperatures developed along a discrete slip surface would continuously dissociate the carbonate rock into a mixture of lime (CaO) and CO<sub>2</sub> gas during travel and the CO<sub>2</sub> gas would provide a lubricant along a basal slip surface.

A mechanical fluidization model in spreading avalanches has been proposed. In this model, the debris avalanche deposits are formed by fluidlike spreading of the debris under the action of gravity, and this spreading occurs due to fluidization of the debris by high basal shear stress as it moves rapidly across the ground. The correlation between volume and the apparent angle of friction is a result of fluidlike spreading of debris avalanches during runout into thin sheets: the larger the volume, the larger the area covered by debris, and the larger the runout length for a given fall height.

A Bingham flow model has been proposed for the Mount St. Helens debris avalanche based on the geomorphology of the Mount St. Helens deposit. The existence of natural levees (Fig. 2B) and marginal and distal cliffs (Fig. 1) suggests non-Newtonian (Bingham) flow behavior. The Bingham flow model has also been used to explain the depositional features and eyewitness of the 1984 debris avalanche, Ontake volcano, Japan. A transport model using initial sliding and later plug (Bingham) flow was proposed after quantitative data were obtained from the Iwasegawa debris avalanche deposit at Tashiro-dake volcano, Japan, and the Kaida debris avalanche deposit at Ontake volcano, Japan.

The granular flow model has also been proposed for

the 1980 Mount St. Helens debris avalanche, based on detailed field evidence of the deposit. The granular flow model has also been used for the debris avalanche at Cantal volcano, France, using anisotropy of magnetic susceptibility (AMS) measurements of the matrix fabric. The data suggest transport of the avalanche by liquefied nonturbulent granular flows. Distally, imbricated deposits suggest more turbulent flow. Emplacement of the avalanche results from progressive aggradation of the particles related to a loss of the nonturbulent liquefied stage. The mass of the avalanche becomes a plug flow that exerts strong friction on the basement.

Another model uses basal low-density layers, based on computer simulation of interacting two-dimensional disks. The basal low-density layer is a region where the particles are very active in the sense that they have large random velocity components (high granular temperature). A basal low-density layer supports an overriding high-density, low-mobility debris "plug" during travel. Computer simulations of granular avalanches were performed using from 5000 up to 1,000,000 two-dimensional disks. The model results suggest that the basal friction coefficient varies with shear rate, where higher shear rates give rise to higher friction coefficients. For debris avalanches with a given fall height to particle diameter ratio, debris avalanches with larger volumes have lower internal shear rates, and thus, lower basal friction coefficients.

Another concept is the mass loss model, which suggests the low apparent angle of friction values achieved by debris avalanches occur because they selectively deposit low-velocity material during movement. The ultimate runout length of a debris avalanche traveling by such a mechanism would depend on the rate and timing of the mass loss. In this model, once a debris avalanche reaches a depositional area, material at the trailing end of the moving avalanche begins to deposit, transferring its energy forward to the moving part of the avalanche. The toe of the avalanche continues to move downslope propelled by the input of momentum from decelerating trailing clasts until the stopping wave catches up with the toe.

A seismic energy fluidization model was given for the 1944 Mount Vesuvius block-and-ash avalanches in Italy. In this model the relative importance of seismic tremor to maintaining avalanche mobility is stressed. A basal pressure wave model has also been suggested where a wave propagated along the basal layer at the phase velocity, which is initially greater than the debris avalanche velocity. With increasing avalanche velocity, the avalanche mass catches up with the guided wave. Over a threshold avalanche velocity, a "sonic boom" is gener-

ated around the basal layer, and the shock contributes to a loosening of the avalanche mass into a fluidized state.

A biviscous flow model has been used to simulate realistic peak velocities and travel times for the 1974 Mayunmarca debris avalanche, Peru, the 1980 Mount St. Helens debris avalanche, United States, and the 1984 Ontake debris avalanche, Japan. Numerical biviscous modeling indicates that the avalanche at Mayunmarca and avalanche I at Mount St. Helens in 1980 ( $H/L \sim 0.2$ ) were of relatively high strength, with apparent Newtonian viscosities of up to several hundred  $m^2/s$ . In contrast, the explosively triggered avalanche II/III flow at Mount St. Helens in 1980 and the Ontake debris avalanche in 1984 ( $H/L \sim 0.1$ ) were of relatively low strength, with apparent Newtonian viscosities 1–2 orders of magnitude lower.

Some combination of these models probably applies in most cases, and each debris avalanche, depending on its composition, cause, volume, and environment, could be simulated by only some of the models listed here.

## VII. EXAMPLES

### A. 1980 Mount St. Helens (Bezmyianny Type)

A swarm of volcanic earthquakes was first detected on March 20, 1980. An initial phreatic explosion occurred on March 27, after 123 years of dormancy. Several phreatic explosions followed and normal faults gradually developed at the summit crater. The north side of the volcanic edifice gradually bulged outward, beginning in early April. Phreatic explosions were repeated and deformation accelerated. A maximum horizontal displacement of 120 m was recorded in the middle of May. Finally, the northern sector of the volcanic edifice collapsed at 8:32 a.m. on May 18. The resulting debris avalanche filled the upper tributary of the Toutle River and traveled up to 28 km away from the source. Its volume was  $2.5 \text{ km}^3$ . The velocity of the avalanche was about 50–70 m/s, judging from a series of photographs. The collapsing mass was affected by a secondary explosion producing a lateral blast and destroying over 500  $\text{km}^2$  of forest area. The maximum velocity of the blast was assumed to be more than 80 m/s. A plinian eruption followed just after the emplacement of the debris avalanche and a pyroclastic flow of  $0.1 \text{ km}^3$  was also emplaced. The climactic eruption was over in the evening of May 18. The total number of fatalities was 57.

Plinian eruptions with pyroclastic flows were produced on several occasions through October 1980 and then a new lava dome began to grow on the floor of the amphitheater. Small-scale explosive eruptions and intrusion of new lobes were repeated until October 1986.

### B. 1888 Bandai (Bandai Type)

The first seismic activity began on July 8, 1888. Continuous seismicity occurred almost every day until the morning of July 15. Then a strong earthquake was felt about 7:30 a.m. on July 15. A series of strong earthquakes followed and finally a phreatic explosion occurred at the summit. After a further 15–20 explosions occurred, the northern sector of the volcano collapsed to produce a debris avalanche. The debris avalanche covered an area of 3.5 km<sup>2</sup> and its volume was 1.5 km<sup>3</sup>. Small-scale explosions followed 30–40 min after the climactic event. The eruption was over by the evening of the same day. The total number of fatalities was 461.

### C. 1792 Unzen (Unzen Type)

A swarm of earthquakes began in November 1791. A magmatic eruption began on February 29, 1792. The volcano produced a dacite lava flow from a vent at the northern slope of Unzen volcano by April 23. Its volume was about 0.03 km<sup>3</sup>. A swarm of tectonic earthquakes occurred simultaneously with the discharge of the lava flow. A small-scale collapse of part of a 4000-year-old lava dome, Mayuyama, located 4 km away from the vent of the new lava, occurred on April 9. A second and climactic collapse was triggered by a relatively large tectonic earthquake ( $M = 6.4$ ) on May 21. The avalanche flowed into Ariake Bay and generated a major tsunami. The total volume of the avalanche was 0.48 km<sup>3</sup>. The total number of fatalities was 15,190, including 11,000 taken by the tsunami.

---

## VIII. CONCLUSIONS

Debris avalanches constitute an only recently recognized form of volcanic phenomena. Hummocky topography, natural levees, marginal cliffs, and distal cliffs characterize young and well-preserved deposits. An am-

phitheater at the source is also a characteristic geomorphic feature. The internal framework that characterizes debris avalanche deposits is composed of debris-avalanche blocks and a debris-avalanche matrix. The former comprises large fractured and deformed fragments mostly derived from the source volcano, preserving original internal structures and textures. The latter consists of a mixture of smaller volcanic fragments derived from various parts of the source volcano and mixed with a minor amount of exotic materials.

Three types of link to eruption processes are defined: debris avalanches associated with intrusion of new magma, those associated with phreatic explosions, and those triggered by earthquakes. The ratio of collapse height to runout distance is generally between 0.2 and 0.06. In some cases, clay-rich debris avalanches may transform into lahars and spread over a much wider area.

The eruption and emplacement of debris avalanches are now recognized as common phenomena during the entire growth history of composite volcanoes. However, the transportation process for debris avalanches is not yet fully understood. The frequency of this type of volcanic activity is lower than the other styles of eruption, but the magnitude of single events is generally large and hazardous. Thus, further work, both theoretical modeling and case studies of deposits, is necessary for the mitigation of volcanic risk.

---

## ACKNOWLEDGMENTS

We greatly appreciate valuable comments by Jonathan Dehn, Vincent E. Neall, and James W. Vallance.

---

## SEE ALSO THE FOLLOWING ARTICLES

Composite Volcanoes • Ignimbrites and Block-and-Ash Flow Deposits • Lahars • Plinian and Subplinian Eruptions • Vulcanian Eruptions

---

## FURTHER READING

Campbell, C. S., Cleary, P. W., and Hopkins, M. (1995). Large-scale landslide simulations: Global deformation, velocities and basal friction. *J. Geophys. Res.* **100**, 8267–8283.

